







# Principal Denudation Processes and Their Contribution to Fluvial Suspended Sediment Yields in the Upper Yangtze River Basin and Volga River Basin

VALENTIN Golosov<sup>1,2,3</sup>, e-mail: golossov@rambler.ru;  0000-0002-4351-8323

ZHANG Xin-bao<sup>1</sup>, e-mail: zxbao@imde.ac.cn;  0000-0002-8616-107x

HE Xiu-bin<sup>1</sup>  e-mail: xiubinh@imde.ac.cn;  0000-0001-6786-1284

TANG Qiang<sup>1,4</sup>, e-mail: qiangtang@rcees.ac.cn;  0000-0003-0861-9943

ZHOU Ping<sup>1</sup>, e-mail: zp09@imde.ac.cn;  0000-0003-4675-2737

*1 Key Laboratory of Mountain Surface Processes and Ecological Regulation, Institute of Mountain Hazards and Environment, Chinese Academy of Sciences, Chengdu 610041, China*

*2 Faculty of Geography, Moscow State University, Moscow 119991, Russia*

*3 Kazan (Volga region) State University, Kazan 420008, Russia*

*4 State Key Laboratory of Urban and Regional Ecology, Research Center for Eco-environment Sciences, Chinese Academy of Sciences, Beijing 100085, China*

**Citation:** Golosov V, Zhang XB, He XB, et al. (2015) Principal denudation processes and their contribution to fluvial suspended sediment yields in the Upper Yangtze River Basin and Volga River Basin. *Journal of Mountain Science* 12(1). DOI: 10.1007/s11629-014-2975-7

© Science Press and Institute of Mountain Hazards and Environment, CAS and Springer-Verlag Berlin Heidelberg 2015

**Abstract:** This paper synthesized the principal land denudation processes and their role in determining riverine suspended sediment yields (SSY) in two typical geographical environments of the Upper Yangtze River Basin in China and the Volga River Basin in Eastern Europe. In the Upper Yangtze River Basin, natural factors including topography, climate, lithology and tectonic activity are responsible for the spatial variation in the magnitude of denudation rates. Human disturbances have contributed to the temporal changes of soil erosion and fluvial SSY during the past decades. On one hand, land use change caused by deforestation and land reclamation has played an important role in the acceleration of sediment production from the central hilly area and lower Jinsha catchment; On the other hand, diverse soil conservation practices (e.g., reforestation, terracing) have contributed to a reduction of soil erosion and sediment production since the late 1980s. It was difficult to explicitly decouple the effect of mitigation measures in the

Lower Jinsha River Basin due to the complexity associated with sediment redistribution within river channels (active channel migration and significant sedimentation). The whole basin can be subdivided into seven sub-regions according to the different proportional inputs of principal denudation processes to riverine SSY. In the Volga River Basin, anthropogenic sheet, rill and gully erosion are the predominant denudation processes in the southern region, while channel bank and bed erosion constitutes the main source of riverine suspended sediment flux in the northern part of the basin. Distribution of cultivated lands significantly determined the intensity of denudation processes. Local relief characteristics also considerably influence soil erosion rates and SSY in the southern Volga River Basin. Lithology, soil cover and climate conditions determined the spatial distribution of sheet, rill and gully erosion intensity, but they play a secondary role in SSY spatial variation.

**Keywords:** Land denudation; Anthropogenic disturbance; Suspended sediment yield; Upper

**Received:** 2 January 2014

**Accepted:** 9 September 2014

Yangtze River; Volga River

## Introduction

Upland soil erosion and riverine suspended sediment transport have greatly intensified during the past decades by the expansion of diverse human activities (e.g., deforestation, land reclamation, grazing, mining, construction activities, and urbanization), which consequently threatens the sustainable use of fertile land resources, reduces crop productivity, deteriorates water quality and degrades aquatic habitats (Walling and Fang 2003; Gao 2008). The situation is even worse in densely-populated agricultural regions where intensive disturbances induced by human activities have exerted great influences on regional soil erosion and riverine suspended sediment delivery. Understanding land denudation processes and assessing the contribution of natural and anthropogenic driving forces to fluvial suspended sediment yields (SSY) affords a theoretical basis for the design and implementation of effective catchment management strategies and mitigation measures for soil conservation and sediment abatement.

Although being spatially distant, the Upper Yangtze River Basin in southwestern China and the Volga River Basin in the Eastern-European Plain represent typical large-scale geographical environments suffering from diverse human disturbances. Both environments are characterized by a sparsely-populated upstream highland area with minimal agricultural activity and a densely populated middle-lower sub-basin with extensive agriculture. Construction of cascade dams since the 1950s has substantially changed channel connectivity and sediment conveyance. Both nature- and human-induced denudation processes are responsible for the change of riverine suspended sediment discharge, and hence may be used to determine the possible intensity of reservoir sedimentation, which is an engineering concern for hydropower plants around the world (Fan and Morris 1992; Palmieri et al. 2001).

In the present study, the effects of natural factors and diverse human activities on the spatiotemporal variation of the intensity of denudation processes in the Upper Yangtze River

Basin and Volga River Basin are comparatively assessed, and the contribution of individual denudation processes to fluvial SSY are evaluated according to an analysis of various factors and the quantitative assessment of some of the processes available for the Upper Yangtze Basin and the Volga River Basin. The main reason for the selection of these two basins is the possibilities to demonstrate the differences of natural factors and human activity influence on erosion rates and suspended sediment yield based on quantitative spatial-temporal data available for both basins (with similar area and spatial distribution of anthropogenic impact).

## 1 Study Area

### 1.1 The upper Yangtze River basin

The Upper Yangtze River originates from the Qinghai-Tibetan highland, extends over a 4300 km main channel to Yichang and drains a catchment of approximately 1.05 million km<sup>2</sup> in southwestern China. It typically comprises four major tributaries. The Jinsha has a main channel of 2316 km (upstream Yibin) and covers a catchment of 128,000 km<sup>2</sup>. The Min-Tuo has a main channel of 793 km, flows into the Yangtze main channel at Yibin from the left bank and collects a watershed of 160,860 km<sup>2</sup>. The Jialing has a main channel of 1119 km, enters the main channel at Chongqing from the left bank and drains a catchment of 160,000 km<sup>2</sup>. The Wu extends over a main channel of 1037 km through the Karst area on the Guizhou Plateau, drains into the Three Gorges Reservoir at Fuling from the right bank and collects a catchment of 87,900 km<sup>2</sup>. There are also many small tributaries that directly drain into the main channel between Yibin and Yichang (Figure 1).

This Basin contains 12 latitudinal degrees (24° N - 36° N) and 22 longitudinal degrees (90° E - 112° E) with an altitude ranging between 100 and 7500 m. The regional landform is characterized by three structural sub-regions: the Qinghai-Tibetan Plateau, the Yunnan-Guizhou Plateau and the Sichuan Depression, which are separated by two tectonically active mountainous areas. Regional land use is substantially determined by population density and local topography. Arable lands are

mainly distributed in the densely-populated central hilly area. The surrounding mountainous region and highland are mainly occupied by woodland and grassland, except for the utmost western high-altitude area, which is wasteland (Figure 2a). Regional climate is dominated by a humid subtropical monsoon and partly influenced by local topography in the western highland. Annual precipitation decreases from 1000-1800 mm in the east to 200-400 mm in the north and west. There is high spatial variation in precipitation, with annual precipitation varying from 200-400 mm on the Qinghai-Tibetan Plateau to more than 2000 mm at Ya'an. The mean annual temperature changes from -4 to +21°C from the West to the East. The land is dominated by Mesozoic detrital rocks (mudstone and red sandstone), Paleozoic sedimentary rocks, igneous rocks (granite and basalt) and metamorphic rocks in the Tibet Plateau (Figure 2b).

1.2 The Volga River Basin

The Volga River, which is entirely located on the Russian Plain (or Eastern European Plain), has a main channel of 3700 km and covers a drainage basin of approximately 1.38 million km<sup>2</sup>. The river channel is almost isometric in the middle reaches but becomes very narrow in the lower reaches (Figure 3). The Volga River Basin is dominated by plain landscapes, with mountainous terrain occupying no more than 5% of the total basin area. Plain landscapes are represented by alternate uplands and lowlands of different origin. Up to 80% of the total basin area is characterized by elevations less than 200 m above sea level. In the uplands the elevation can reach 300-400 m, and a maximum of 700 m at the Kara-Tau Ridge. The main rivers of the Volga River Basin are incised to 50-200 m depth relative to the main interfluvies in most parts of the basin area. In the uplands, the incision

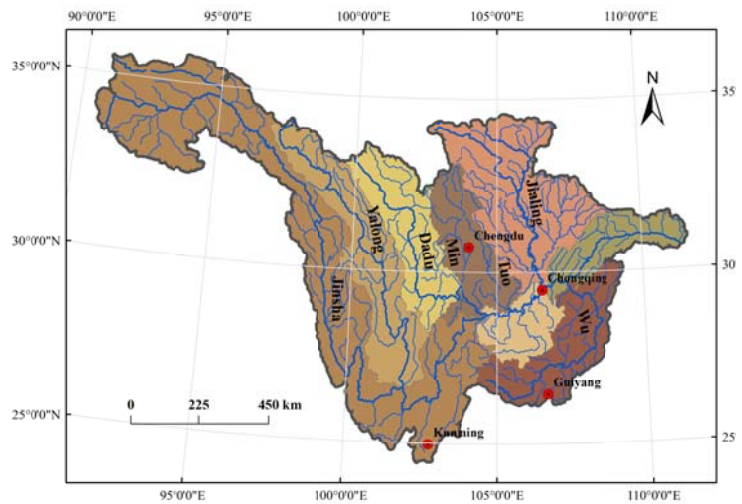


Figure 1 Geographical map of the Upper Yangtze River Basin in southwestern China.

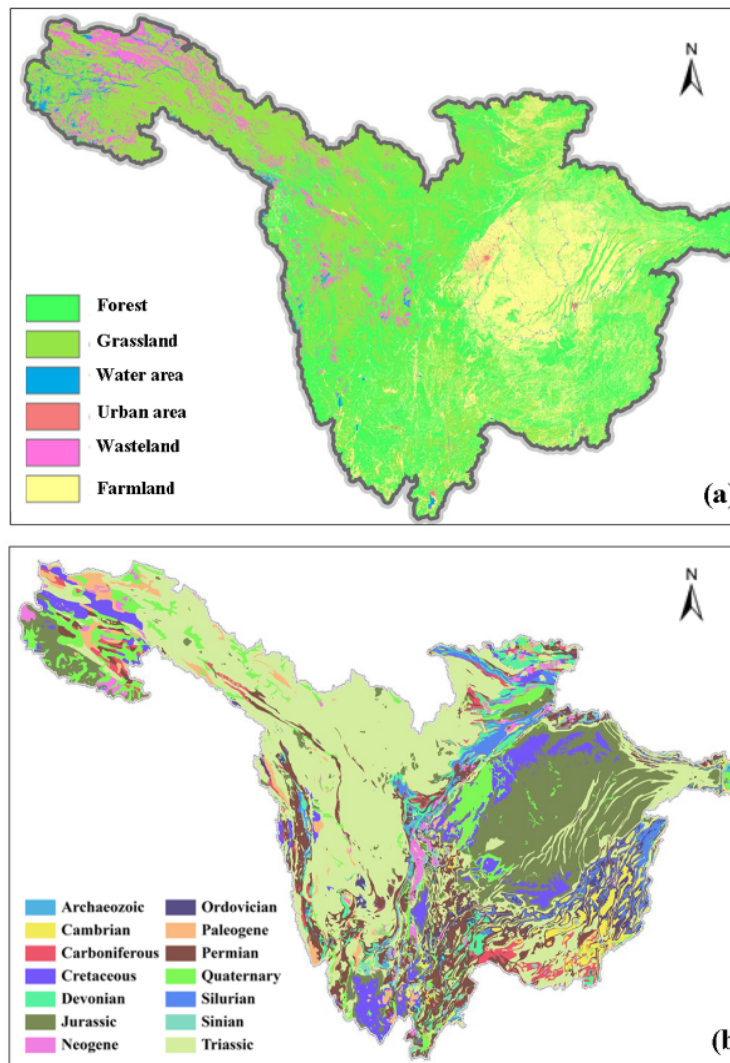


Figure 2 The characteristics of (a) land use and (b) geology in the Upper Yangtze River Basin.

depth of the main rivers can reach 150-200 m. However, the dominant topographical range between the main interfluvies and the river valley bottoms is 50-100 m.

There are two main tributaries of the Volga River: the Oka River, with a basin area of 245,000 km<sup>2</sup> and the Kama River, with a basin area of 507,000 km<sup>2</sup>. The average annual temperature changes from 3.0°C in the North to 9.0°C in the South based on landscape changes from forest (taiga) to semi-desert (Figure 4a). The average annual precipitation decreases from 750 mm to 150 mm from the North to the South. During the winter (December-March) the majority of the precipitation is snow. Spring snowmelt waters contribute most to the Volga River's annual discharge. In different parts of the river basin the contribution of snowmelt waters varies from 50% to 65%, being about 60% on average for the entire river basin. The soil types in the Volga River Basin are distributed according to the spatial distribution of parent rocks and climate condition changes (Figure 4b) (Gavrilova



**Figure 3** Geographical map of the Volga River Basin on the Russian Plain.

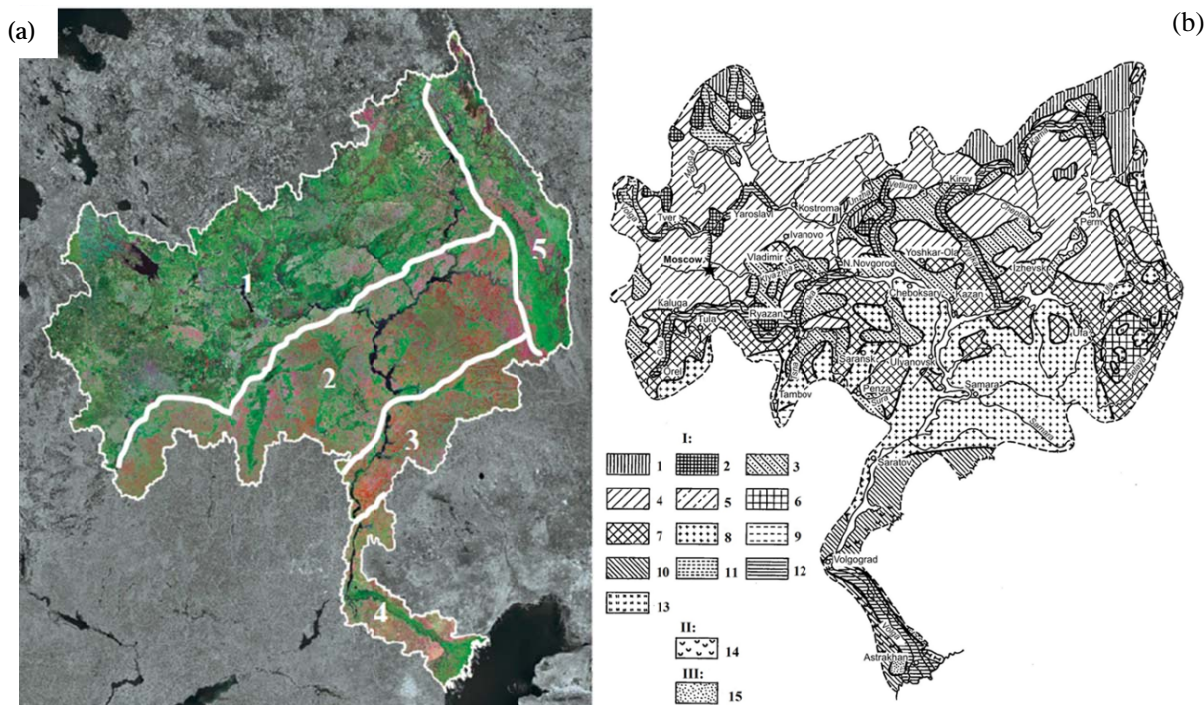


**Figure 4** (a) Landscape map of the Volga River basin. 1) forest, 2) forest-steppe, 3) steppe, 4) semi-desert and 5) Ural mountains; (b) Soil cover map of the Volga River Basin. Soil types: 1) podzolic; 2) gley podzolic; 3) podzols and iron-rich soddy podzolic soils; 4) soddy podzolic soils; 5) initially carbonate soddy podzolic soils; 6) brown forest soils; 7) gray forest soils; 8) chernozem soils; 9) dark humus soils; 10) chestnut soils; 11) peat and peat gley soils; 12) alluvial soils; and 13) mountainous dark humus soils. Soil complexes: 14) solonetz soils. Non-soil surface materials: 15) sands.

and Bogdanova 1998). Glacial deposits occupy the northern part of the basin and loam loess dominates in the southern part.

Before the reservoir cascade construction, the Volga River annually exported large volumes of transported matter into the Caspian Sea, approximately equal to  $26 \times 10^6$  t of suspended sediment and  $45 \times 10^6$  t of dissolved materials. The respective SSY are  $19 \text{ t}\cdot\text{km}^{-2}\cdot\text{yr}^{-1}$  for suspended sediment and  $33 \text{ t}\cdot\text{km}^{-2}\cdot\text{yr}^{-1}$  for dissolved materials. Presently, sediment entrapment by large reservoirs has resulted in a decreased SSY at the basin outlet ( $8 \times 10^6 \text{ t}\cdot\text{yr}^{-1}$ ). Meanwhile, a general increase in water pollution has caused a dramatic increase in dissolved material yield ( $65\text{-}70 \times 10^6 \text{ t}\cdot\text{yr}^{-1}$ ) (Gavrilova and Bogdanova 1998).

## 2 Materials and Methods

Datasets concerning upland soil erosion and riverine SSY were assembled in the present study. Long-term records of riverine water discharge and sediment load at major gauging stations in the Upper Yangtze River Basin are available from the Ministry of Water Resources of China (<http://www.mwr.gov.cn>).

mwr.gov.cn).

The data of soil erosion rates on experimental runoff plots at spatially-distributed observation stations have been collected since the mid-1980s. Unfortunately, methodological and technical errors were made at the beginning, leading to incorrect results during the first two years of observation (Table 1). The results obtained on runoff plots have been reasonable since 1986, but opinions on the extremely high erosion rates on cultivated fields in the Upper Yangtze River Basin appear to be based on those initial results (Shi 1998; Yin et al. 1998; Yang et al. 2003; Wang et al. 2004). The results of recent observations of runoff plots (Lin et al. 2009) and small catchments (Yang et al. 2009) demonstrate much lower rates of soil losses, but the duration of the given observations has been too short to characterize the mean erosion rates for a relatively long time period.

It is possible to exclusively use indirect methods to assess the mean annual soil redistribution rates on cultivated fields, uncultivated slopes and small slope catchments for the period since 1963. The  $^{137}\text{Cs}$  tracing technique affords a simple means for evaluating soil erosion and sediment redistribution rates since 1963, and

**Table 1 Soil erosion observation on runoff plots in the Sichuan Basin (The office of soil and water conservation committee of Sichuan Province 1991)**

Year (runoff times)	Precipitation during runoff events (mm)	Runoff index	Runoff depth(mm)	Soil erosion rates ( $\text{t}\cdot\text{km}^{-2}\cdot\text{yr}^{-1}$ )	Annual precipitation(mm)
<b>Plot 5° (sloping cultivated land; crops: sweet potato + wheat )</b>					
1984 (6)	406.1	0.11	46.5	4485.2	654.9
1985 (12)	642.1	0.3	194.4	3700.9	1243
<b>1986-1989</b>					
<b>Plot 10° (sloping cultivated land; crops: sweet potato + wheat)</b>					
1984 (11)	499.1	0.12	57.8	8764.9	654.9
1985 (12)	642.1	0.26	170.2	5115.1	1243
<b>1986-1989</b> No runoff and sediment were detected					
<b>Plot 15° (sloping cultivated land; crops: sweet potato + wheat )</b>					
1984 (12)	510.6	0.14	69.4	13,343.3	654.9
1985 (12)	642.1	0.41	260.0	8744.2	1243
1986 (1)	124.9	0.11	14.1	211.6	911.2
1987 (1)	124.9	0.10	12.8	100.5	884.6
<b>1988-1989</b> No runoff and sediment were detected					
<b>Plot 20° (sloping cultivated land; crops: sweet potato + wheat )</b>					
1984 (11)	493.1	0.11	55.1	17,504.4	654.9
1985 (12)	642.1	0.34	220	11,619.2	124.
1986 (1)	124.9	0.04	43.3	66.5	911.2
1987 (1)	124.9	0.1	12.2	190.6	884.6
<b>1988-1989</b> No runoff and sediment were detected					
<b>Plot 25°</b>					
1984 (12)	510.6	0.14	70.3	23,563.8	654.9
1985 (12)	642.1	0.3	194.8	15,895.3	1243
1986 (2)	222.8	0.23	45.4	733.2	911.2
1987 (1)	124.9	0.28	34.9	408.2	884.6
<b>1988-1989</b> No runoff and sediment were detected					

Plot 5°下面的 **1986-1989** 后面没有数字也没有注释, 是不是和 Plot 10°中的 1986-1989 一样情况? !

Plot 25°后面没有注释,是不是和前面一样的情况?!如果是的话,这些注释可以在表后注明即可,表中的可删掉。

has been widely used around the world in the quantitative assessment of soil loss/gain in cultivated fields (Sutherland 1992; Zhang et al. 1998, 2008; Walling et al. 1999; Walling et al. 2000; Schuller et al. 2004; Li et al. 2007; Belyaev et al. 2009) and uncultivated lands (Mabit et al. 2008; Porto et al. 2011). It is necessary to note that the values of soil losses or gains obtained using the  $^{137}\text{Cs}$  tracing technique represent the gross effect of water, wind and tillage erosion in addition to soil loss from the harvesting of root crops (Ritchie and McHenry 1990; Tiessen et al. 2009). In the case of the Upper Yangtze River Basin, water erosion prevails under the hypothesis that the relative contribution of wind erosion and soil loss from harvesting is extremely low. Tillage erosion considerably influences the soil redistribution rate within cultivated terraces (Quine et al. 1999), but it does not significantly affect net soil losses. Detailed studies of tillage erosion processes within cultivated terraces have shown that there are no net soil losses (Su et al. 2010). Investigations of soil redistribution rates using the  $^{137}\text{Cs}$  technique have been undertaken in different parts of the Upper Yangtze River Basin (Tables 2 and 3) (Wang et al. 2003; Wen et al. 2005, 2008, 2011; Qi et al. 2006; Zhang et al. 2011).

Mean annual rate of soil losses at catchment

scale were determined based on an evaluation of sediment volume collected in small ponds in small catchments that had sustained a well-known period of exploration. Such ponds are located in the slope catchment outlet and serve as sediment traps for the majority of the soil that erodes from the catchment area. Sediment volumes were determined for 62 small ponds located within the Sichuan Hilly Basin in the central area.

Long-term averaged soil erosion rates in the Volga River Basin were assessed through the combined application of a modified version of the Universal Soil Loss Equation (USLE) to evaluate soil loss from rainfall (Larionov 1993) and the model used by the Russian State Hydrological Institute (Instruction on calculating hydrological characteristics for planning counter-erosion measures in the European area of the USSR, 1979) to assess soil loss during snowmelt (Figure 5a). Model calculations were verified using field measurements of sediment storage in small field ponds, and showed good results (Litvin et al. 2003). All parameters included in USLE were calculated based on Russian Meteorological Survey data (for erosion index of precipitation), Russian Soil Map (soil erodibility), and results of measurements of LS factor on topographical maps with scale 1: 25,000. A detailed description about data

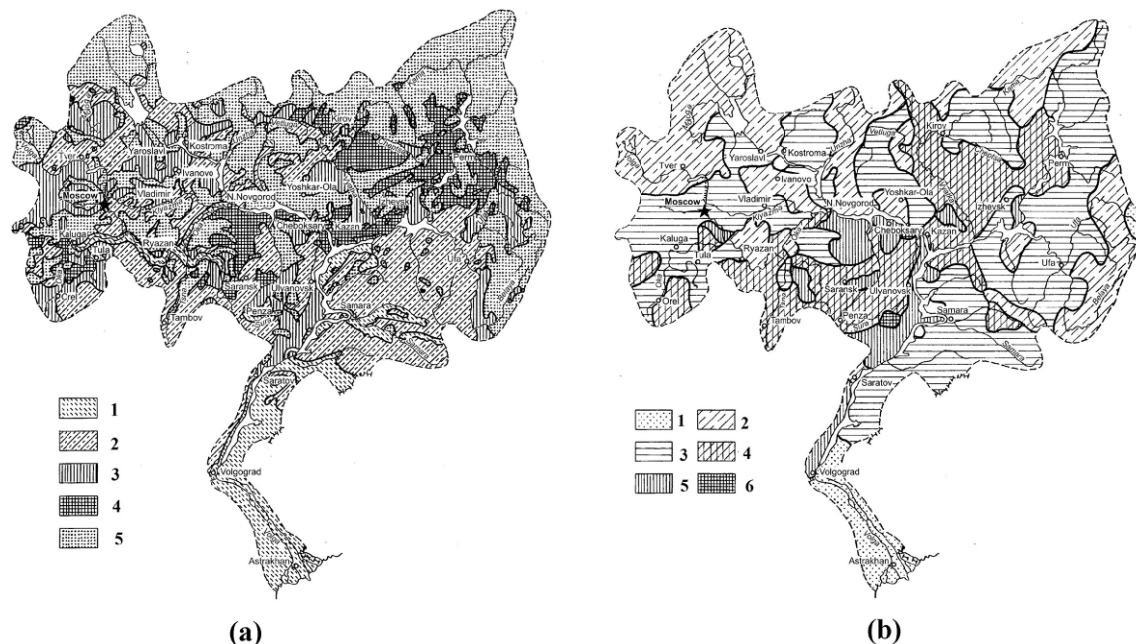


**Figure 5** (a) Average annual soil erosion rates for arable land in the Volga River Basin: 1:  $< 1 \text{ t}\cdot\text{ha}^{-1}\cdot\text{yr}^{-1}$ ; 2:  $1\text{-}5 \text{ t}\cdot\text{ha}^{-1}\cdot\text{yr}^{-1}$ ; 3:  $5\text{-}10 \text{ t}\cdot\text{ha}^{-1}\cdot\text{yr}^{-1}$ ; 4:  $10\text{-}20 \text{ t}\cdot\text{ha}^{-1}\cdot\text{yr}^{-1}$ ; and 5: forests and bogs. (b) Average annual intensity of sediment production by gully erosion in the Volga River Basin: 1:  $< 0.1 \text{ m}^3\cdot\text{km}^{-2}\cdot\text{yr}^{-1}$ ; 2:  $0.1\text{-}1.0 \text{ m}^3\cdot\text{km}^{-2}\cdot\text{yr}^{-1}$ ; 3:  $1.0\text{-}20.0 \text{ m}^3\cdot\text{km}^{-2}\cdot\text{yr}^{-1}$ ; 4:  $20.0\text{-}75.0 \text{ m}^3\cdot\text{km}^{-2}\cdot\text{yr}^{-1}$ ; 5:  $75.0\text{-}200.0 \text{ m}^3\cdot\text{km}^{-2}\cdot\text{yr}^{-1}$ ; and 6:  $>200 \text{ m}^3\cdot\text{km}^{-2}\cdot\text{yr}^{-1}$ .

**Table 2** Soil erosion rates on cultivated land obtained using  $^{137}\text{Cs}$  tracing technique

Region	Location	Precip. (mm)	Land type	Slope length (m)	Slope angle (°)	Soil	$^{137}\text{Cs}$ reference inventory ( $\text{Bq}/\text{m}^2$ )	$^{137}\text{Cs}$ effective reference inventory ( $\text{Bq}/\text{m}^2$ )	$^{137}\text{Cs}$ content ( $\text{Bq}/\text{m}^2$ )		No. of profile	ASER ( $\text{t}\cdot\text{km}^{-2}\cdot\text{yr}^{-1}$ )
									Range	Aver.		
The Lower Jinsha-Jiang River Basin	Muding	850.6	CS_L terrace	13	20	P_soil	919.8	643.9	88.0-488.0	204.9	14	6271
				10	0	P_soil		919.8	815.5-1056.3	915.8	5	No erosion
	Zhenba	917	CS_L terrace	21	25	P_soil	1510.4	1057.3	84.8-632	326.1	8	8543
				10	0	P_soil	1510.4	1510.4	1338.2-1636.7	1523.8	4	No erosion
	Zhenbay	613.8	CS_L	25	15	R_soil	620.9	558.8	229.3-773.1	367.6	13	2740
				70	5			558.8	338.0-567.0	425.3	8	1405
The Three Gorge Reservoir Region	Zhigui	1048	CS_L	29	31	Clayey soil	2377.2	1664.0	160.1-2906.5	1340.7	9	2059
				10	25				125.0-927.6	382.5	4	9452
	Zhenba	? ?	CS_L	5	25	P_soil	1924.6	1347.2	13.0-1202.3	499.3	3	7481
				8	25				161.0-692.6	362.2	4	9854
				10	0				1924.6	1050.4-3080.7	1875.1	4
The Middle and Lower Jialing River Basin	Nanchong	1000	CS_L=	17	0-11	P_soil	2035.8	1425.1	28.5-2378.6	709.5	5	4663
				9	5			1730.4	312.0-2286.4	1443.4	4	758
				24.7	14			1425.1	439.5-693.4	528.2	5	6780
	Zhenba	1250	CS_L=	27	10	Y_soil	2375.0	1662.5	86.8-1119.8	513.9	16	7467
				54	34			2137.5	863.5-2784.6	1847.7	17	985
				8	7			2018.8	541.5-1827.0	850.4	8	4200
The Upper Jialing River Basin	Tianshui	605.7	CS_L=	20	19.3	Loess	2573.2	2573.2	111.0-2606.5	885.9	6	4598
				19	18				137.9-1681.2	761.6	6	5310
				34	12.8				245.6-3479.6	1318.9	9	2864
				15	31				207.9-690.5	408.7	4	8216
				25	0				1845.7-3410.7	2675.4	4	No erosion

**Notes:** ASER means Average soil erosion rates. CS\_L= Cultivated sloping land; P\_soil=Purple soil; R\_soil=Dry red soil; Y\_soil=Yellow soil.

**Table 3** Soil erosion rates from uncultivated lands based on application of <sup>137</sup>Cs tracing technique.

Region	Location	Precipi. (mm)	Land type	Slope length (m)	Slope angle (°)	Soil	Vegetation coverage (%)	<sup>137</sup> Cs reference inventory (Bq/m <sup>2</sup> )	<sup>137</sup> Cs content (Bq/m <sup>2</sup> )		No. of profile	ASER (t·km <sup>-2</sup> ·yr <sup>-1</sup> )
									Range	Aver.		
The Lower Jinsha-Jiang River Basin	Muding	850.6	F_L	63.5	14	P_soil	90	919.8	782.7-1227.1	967.1	6	No erosion
	Yiliang	800	F_L	25	5	P_soil	80	1510.4	1460.9-1542.6	1516.5	3	No erosion
	Yuanmou	613.8	G_L	20	21	R_soil	60	620.9	38.8-663.3	329.7	5	876
			G_L	30	30	90	620.9	576.0-1159.9	821.5	6	No erosion	
The Three Gorge Reservoir Region	Zigui	1048	F_L	53	25	P_soil	90	2377.2	65.7-1495.4	960.8	6	310
			F_L	25	25	P_soil	80	2377.2	531.8-1473.8	962.6	5	306
	Kaixian	1200	G_L	3.5	25	P_soil	60	1924.6	798.1-942.0	869.7	3	688
The Middle and Lower Jialing River Basin	Nanchong	1000	G_L	5	5	P_soil	30	2035.8	107.7-124.6	119.0	3	4435
	Zhenba	1250	F_L	82	10	Y_soil	90	2375.0	1065.1-3993.8	2301.4	12	No erosion
The Upper Jialing River Basin	Tianshui	605.7	F_L	30	20.4	Loess	40	2573.2	1308.4-3038.3	2071.5	6	588
				32	22.6				2212.3-3106.5	2560.3	6	No erosion

**Notes:** ASER means Average soil erosion rates. F\_L=Forest land; G\_L=Grass land; P\_soil=Purple soil; R\_soil=Dry red soil; Y\_soil=Yellow soil.



collection, analysis and calculation can be found elsewhere (Larionov 1993; Litvin 2002; Litvin et al. 2003).

One of the parameters that can be used to quantitatively characterize gully erosion's contribution to sediment redistribution within a fluvial system is the area-specific sediment yield  $W_g$ , i.e. volume of sediment delivered from a gully mouth over a unit of time divided by a gully catchment area ( $\text{m}^3 \cdot \text{km}^{-2} \cdot \text{yr}^{-1}$ ). This parameter characterizes the amount of sediment delivered from gullies into the larger elements of a fluvial network (Rysin 1998):

$$W_g = D_g V_g F \quad (1)$$

where  $D_g$  is the gully density,  $1 \cdot \text{km}^{-2}$ ;  $V_g$  is the average rate of gully headcut growth,  $\text{m} \cdot \text{yr}^{-1}$ ; and  $F$  is the average gully cross-section area, m.

The calculation of area-specific sediment yield from gullies ( $W$ ) was carried out for the basins of the first-order rivers as distinguished on the 1:25,000 scale topographical maps. A map of the area-specific sediment yield from gullies was created for the Volga River Basin territory using the results of that calculation (Figure 5b). The map provides the generalized quantitative characteristics of the present-state gully network and records its developmental activity. It also helps to determine the types of territories with different intensities of sediment export from gullies.

The SSY for the small and mid-sized rivers in the Volga River Basin was estimated using the empirically established relationships between water ( $Q$ ) and suspended sediment ( $R_s$ ) discharges measured at certified gauging stations belonging to the Russian Hydrometeorological Service (Chalov and Shtankova 2003). The hydrologic data observed at many stations was used for analysis, and maps illustrating the spatial patterns of river sediment yield within the Volga River Basin were created. These include a map of the average annual suspended sediment concentration (SSC) (Figure 6a) and a map of the average annual suspended sediment yield (ASSY) (Figure 6b)

### 3 Results and Discussion

#### 3.1 The upper Yangtze River basin

Soil erosion rates on cultivated hillslopes was estimated to range between 758 and 9854  $\text{t} \cdot \text{km}^{-2} \cdot \text{yr}^{-1}$ , while that on flat terrace fields was close to 0 in the Upper Yangtze River Basin. The severity of soil erosion on cultivated hillslopes is closely related to slope gradients and soil texture that maximum soil losses occurred on slopes of  $25^\circ$  consisting of purple clay soil. However, the total area of steep cultivated slopes is very small compared with the area of slope catchments. The total area of sloping cultivated land is 8.67 million ha ( $>5^\circ$ ) across the Upper Yangtze River Basin, which is less than 9%

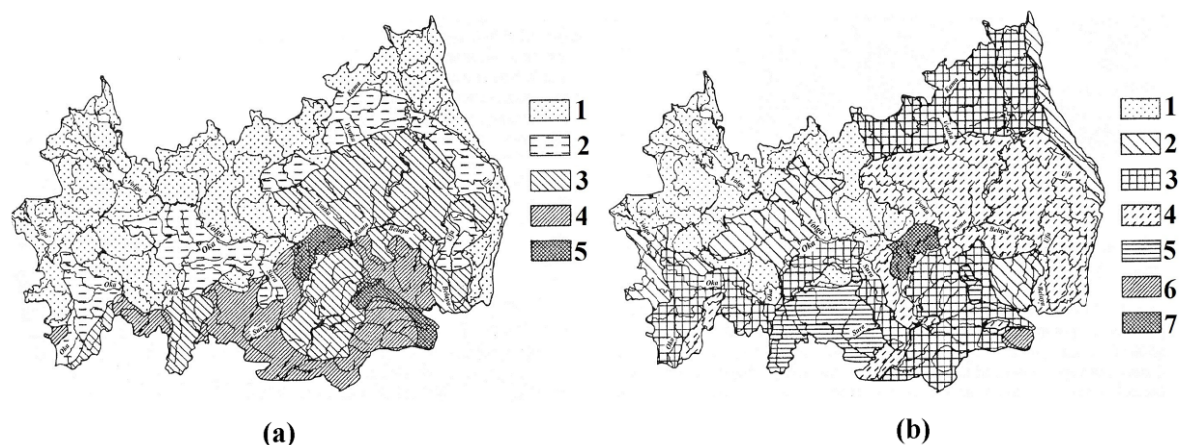


**Figure 6** (a) Average annual suspended sediment concentration in rivers of the Volga River Basin (without the lowest Volga reach) (Chalov and Shtankova, 2003). The SSC value intervals are: 1:  $<50 \text{ g} \cdot \text{m}^{-3}$ ; 2:  $50\text{-}100 \text{ g} \cdot \text{m}^{-3}$ ; 3:  $100\text{-}200 \text{ g} \cdot \text{m}^{-3}$ ; 4:  $200\text{-}500 \text{ g} \cdot \text{m}^{-3}$ ; and 5:  $>500 \text{ g} \cdot \text{m}^{-3}$ . (b) Average area-specific annual suspended sediment yield in rivers of the Volga River Basin (without the lowest Volga reach) (Chalov and Shtankova 2003). The SSY value intervals are: 1:  $<5 \text{ t} \cdot \text{km}^{-2} \cdot \text{yr}^{-1}$ ; 2:  $5\text{-}10 \text{ t} \cdot \text{km}^{-2} \cdot \text{yr}^{-1}$ ; 3:  $10\text{-}20 \text{ t} \cdot \text{km}^{-2} \cdot \text{yr}^{-1}$ ; 4:  $20\text{-}30 \text{ t} \cdot \text{km}^{-2} \cdot \text{yr}^{-1}$ ; 5:  $30\text{-}40 \text{ t} \cdot \text{km}^{-2} \cdot \text{yr}^{-1}$ ; 6:  $40\text{-}60 \text{ t} \cdot \text{km}^{-2} \cdot \text{yr}^{-1}$ ; and 7:  $>60 \text{ t} \cdot \text{km}^{-2} \cdot \text{yr}^{-1}$ .

of the total area of the Upper Yangtze Basin. Usually it does not exceed 10%-25% from the slope catchment area, even in the Sichuan Hilly Basin, which represents the main agricultural region of the Upper Yangtze River Basin (Table 4).

Soil erosion rates on the forest and grass lands were estimated to range between 0 and 4435 t·km<sup>-2</sup>·yr<sup>-1</sup>. Vegetation coverage exerted the most important influence on soil erosion on uncultivated slopes. The maximum soil losses were on grass slopes with vegetation cover of less 30%. On all the other uncultivated slopes, soil losses were less than 1000 t·km<sup>-2</sup>·yr<sup>-1</sup> (Table 3).

Catchment average soil losses ranged from 80 to 1568 t·km<sup>-2</sup>·yr<sup>-1</sup> following the distribution of studied catchments according to sediment yield (Figure 7). The soil losses include erosion from cultivated land sediment and barren land, and gully bank and bottom erosion. The high variability of sediment yield between catchments can be explained by the different proportions of arable lands and differences in the loss of soil with different grain size compositions. The majority of the sediment eroded from small catchments in the Sichuan Hilly Basin and was delivered to the river channels. Riverine SSY can thus be used as a direct indicator of soil loss changes in the Sichuan Hilly Basin.

Cultivated lands do not exceed 30% of the Upper Yangtze River Basin, except for the Sichuan Hilly Basin area (Table 4). Furthermore, the proportion of cultivated lands varies from 5%-15%. The majority of the arable land is located along the river valleys, and most of the eroded sediment can be transported directly to the river channels during rainstorm events. However, the lack of correlation between cultivated lands and suspended SSY for the rivers of the Lower Jinsha Basin (Higgitt and

Lu 2001) is good confirmation that sediment eroded from cultivated lands is not the main sediment source. Good correlation was found between these parameters for the Oka River Basin, where soil losses from cultivated lands are the main sediment source (Golosov 2006).

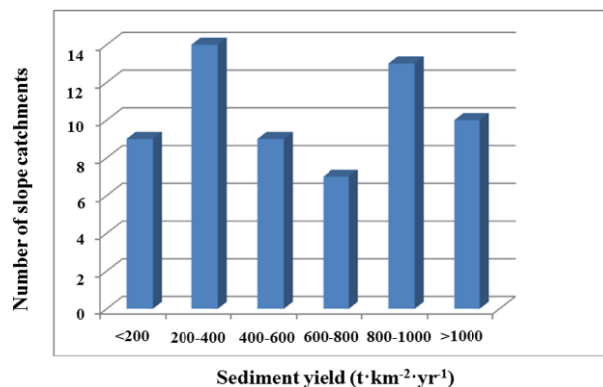


**Figure 7** Distribution of small slope agricultural catchments classified by mean annual sediment yield.

The intensity of denudation directly depends on the intensity of weathering in mountain areas. Both physical and chemical weathering is intensive in the Upper Yangtze River, allowing the intensification of gravitational processes on the steep slopes, including landslide formation. The Lower Jinsha River Basin is located in the very active orogenic belt, which is characterized by a high recurrence of earthquakes. The exposed source rocks are easily weathered under favorable weathering conditions and transported rapidly from the slope to the valley. Moreover, the quick transportation of weathering products further increases the exposure of fresh rocks and consequently contributes more to the silicate weathering of the source rocks (Edmond et al. 1995). A significant association between silicate chemical weathering and physical erosion can be

**Table 4** Proportion of cultivated land areas with various gradients from the total cultivated land area for different parts of the Upper Yangtze River basin.

Region	Area (10 <sup>4</sup> km <sup>2</sup> )	Proportion of area for a certain gradient to total cultivated land area				Proportion of total cultivated land area to the territory
		< 5°	5°-15°	15°-25°	>25°	
Hilly Sichuan Basin	10.5	0.6	0.20	0.15	0.05	0.4-0.6
Mountain area around the Sichuan Basin	20.9	0.3	0.32	0.25	0.13	0.1-0.25
Loessic mountain	4.1	0.3	0.3	0.22	0.18	0.1-0.15
Hengduan Mountains	19.6	0.35	0.24	0.18	0.13	0.05-0.15
Lower Jinsha River mountain	7.2	0.3	0.3	0.2	0.2	0.05-0.25
Tibet Plateau	30.2	0.8	0.19	0.01	0	<0.01
Karst Plateau	7.5	0.2	0.4	0.3	0.1	0.2-0.3

observed ( $R^2 = 0.89$ ) (Wu et al. 2008), indicating that the chemical weathering in the Jinsha River Basin is controlled by the physical erosion. However, the weathering in the Jinsha Basin is not strong enough to greatly affect K-feldspar, compared with some large tropical rivers, and losses of Ca, Na and Sr are the main form of silicate weathering. Observations have supported the classic viewpoint that climate is the predominant factor controlling the silicate weathering in the Upper Yangtze River Basins (Yang et al. 2004). Debris flows are responsible for sediment transport from first order catchments to the main river valleys. Based on direct observation in the Xiaojiang River Basin, the majority of debris flow basins are located within an elevation range of 700-1500 m and have an area of <math> < 5 \text{ km}^2 </math> (He et al. 2003). The intensive gravitational processes (rock fall, scree) are widespread here due to the extensive physical weathering of rocks on the steep barren slopes of small valleys with high gradient bottoms. The intensity of weathering in particular increases due to fractured rocks and favorable climate conditions, including high day-night and seasonal temperature gradients and intense rainstorms. Moreover, the lower Jinsha Basin is located in an area with a high recurrence of earthquakes, which makes landslides and rock falls widespread.

An active contemporary tectonic processes belt surrounds the Sichuan Hilly Basin from the West, Northwest and North within the zone, with absolute elevations of 1000-2000 m a.s.l.. Combined with intense weathering, specific processes prompt the intensification of different gravitational processes, particularly landslides and rock falls (Jin et al. 2009). However, the recurrence of debris flows is lower here compared with the southern part of the Lower Jinsha River.

The middle and high mountainous regions (2000-4000 m) located between the Qinghai-Tibet Plateau and the Lower Jinsha River Basin in the West are characterized by a cold and relatively dry climate with the main sediment production area in a glacial zone with very active physical weathering. Thus, the highest sediment concentrations are found in the upstream parts of rivers in the given region (Qin et al. 2006), mainly the right-hand tributaries of the Dadu and Yalong Rivers and the middle reach of the Jinsha River Basins. The Middle and Upper Jinsha River Basins are not

affected by anthropogenic influence due to very low population densities. A very good correlation between water discharge and sediment concentration is confirmed for the Yalong and Jinsha Rivers at the Panzhihua since the beginning of the observation (Figure 8).

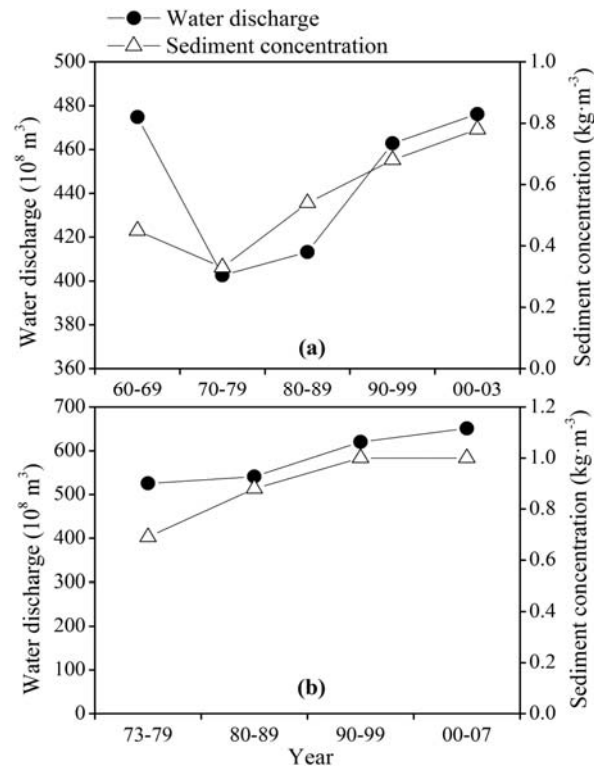


**Figure 8** Temporal dynamic of mean water discharge and sediment concentrations for period of observation (location of gauging station in Figure 8A): (a) Luning station (Yalong River), controlling area-108,100  $\text{km}^2$ ; (b) Panzhihua station (Jinsha River), controlling area-285,000 $\text{km}^2$ .

A completely different situation was observed in the area of carbonate rocks (karst area) occupying the southeastern part of the Upper Yangtze Basin, which belongs to the Wu River Basin. Chemical weathering is dominant there, with almost no surface runoff due to shallow soils and carbonate mother rocks with very high infiltration rates (Peng and Wang 2012). Only the upper part of the Wu River Basin lying outside of the karst is the main sediment production area due to high physical weathering and intensive gravitational processes. The SSY of the Wu River can be used as an indicator of suspended sediment formation from the area located within low mountains (700-1000 m a.s.l.) due to the lack of sediment input from anthropogenic and river-bank

erosion, as a main sediment source.

The lithological factor is also responsible for the high intensity of denudation in the upper Jialing River Basin because it is an easily eroded loess area. The intense destruction of loess was observed under natural conditions due to rainstorm runoff that led to significant gully erosion. In addition, the physical weathering of gully walls is particularly intensive during the cold season when the temperature very often passes through 0°C in a single day, increasing deepening the loess aggregate destruction and scree processes (Golosov and Panin 1988). This area also features high contemporary tectonic activity.

SSY in the Upper Yangtze River mainly originates from the regions with complex topography and intensive human disturbances. There are a great variety of controlling factors that determine the denudation rates and SSY variability. Expansion and intensification of diverse human activities have affected regional soil erosion and riverine suspended sediment delivery since the 1950s (Shi 1998; Yin et al. 1998; Yang et al. 2003; Wang et al. 2004). Forest coverage had decreased by 7%-13% during the 1950s and 1980s due to extensive forest harvesting for fuel consumption and land reclamation (Chen 1996). It was estimated that 35% of the basin area is affected by

soil erosion, which has resulted in water quality deterioration and riparian ecosystem degradation (Wen et al. 2002). However, the relative contributions of human and nature-induced denudation processes to fluvial SSY in the Upper Yangtze River Basin have been inadequately studied. According to the hydrologic data recorded at river gauging stations, the Jinsha and Jialing Basins are the predominant source area for sediment production. However, high SSY in the Jinsha Basin may be ascribed to complex landforms, tectonically active slopes and the intensive human disturbances (e.g., constructional activities, mining), whereas high SSY in the Jialing Basin may be attributed to intensive cultivation on sloping arable lands (Zhang and Wen 2002).

To clarify the influences of both natural and anthropogenic agents on the principal denudation processes in the Upper Yangtze River Basin, the area is divided into seven sub-regions with contrasting behavior and land denudation intensity (Figure 9, Table 5). The classification considered local characteristics of relief, land use, climate and geology (including lithology and tectonic). Each region is characterized by different SSYs (Figure 9) and/or different inputs of denudation processes to SSYs (Table 6).

A major proportion of the suspended sediment

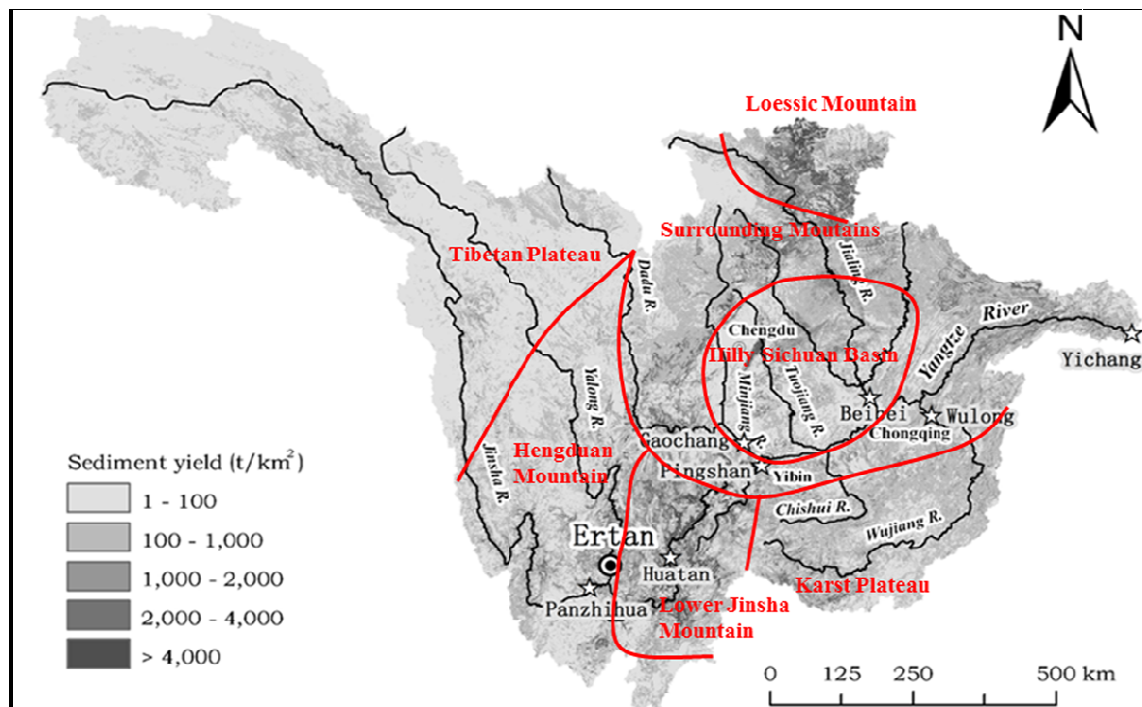


**Figure 9** Regions with different denudation rate intensities and map of SSY for the Upper Yangtze River Basin.

<b>Table 5 Characteristics of regions with different contribution of natural and anthropogenic denudation processes.</b>							
<b>Sub-regions</b>	<b>Area (10<sup>4</sup> km<sup>2</sup>)</b>	<b>Relief</b>	<b>Geology</b>	<b>Climate</b>	<b>Population density (people·km<sup>-2</sup>)</b>	<b>Forest coverage (%)</b>	<b>Arable land ratio</b>
Hilly Sichuan Basin	10.5	Hills with elevation between 200-500 m	Horizontal bedding Mesozoic sedimentary rocks	Eastern Asia Subtropical climate with annual precipitation between 900 mm-1100 mm and mean temperature of 14-16°C.	400-700	15-30	0.4-0.6
Surrounding mountain area	20.9	Low-medium mountains with elevation between 500->2000 m	Paleozoic and Mesozoic sedimentary rocks, a few crystalline rocks. Folds and faults are well developed	Eastern Asia Subtropical climate. annual precipitation: 1000mm-1800 mm; mean temperature: 12-15°C.	100-300	20-40	0.1-0.25
Loessic mountain	4.1	Low-medium mountains. Elevation:600 m->2000 m	Paleozoic sedimentary rocks, a few crystalline rocks covered with loess deposits. Folds and faults are well developed	Eastern Asia Subtropical climate. Annual precipitation: 600 mm-860 mm; mean temperature:11°C -13°C.	100-150	20-40	0.1-0.15
Hengduan Mountains	19.6	Medium-high mountains. Elevation: 1000 m->3500 m	Paleozoic and Mesozoic sedimentary rocks, a few crystalline rocks and protozoa metamorphic rocks. Folds and faults are well developed	Subtropical mountain climate with dry and warm valleys and cold and wet mountains. annual precipitation: 500mm-1600 mm; mean temperature: <0°C-15°C	50-100	20-40	0.05-0.15
Lower Jinsha mountain	7.2	Deeply dissected Medium-high mountains. Elevation: 500 m->3500 m	Paleozoic and Mesozoic sedimentary rocks, a few crystalline rocks and protozoa metamorphic rocks. faults are well developed and very active	Subtropical mountain climate with dry and warm valleys and cold and wet mountains. annual precipitation: 500 mm-1100 mm; mean temperature: 10°C-21°C.	50-200	10-35	0.05-0.25
Tibet Plateau	30.2	High plateau. Elevation:>3500 m	Mesozoic metamorphic rocks and crystalline rocks, a few Paleozoic sedimentary rocks. Folds and faults are well developed	Sub-frigid plateau climate. annual precipitation: 200 mm-700 mm; mean temperature: -4 °C - 6 °C.	1-10	<5	<0.01
Karst Plateau	7.5	Plateau. Elevation: 1000 m-1500 m	Paleozoic- Triassic carbonate rocks, mostly horizontal bedding	Subtropical plateau climate precipitation: 1000 mm-1400 mm; mean temperature: 13 °C -15 °C.	200-300	15-35	0.2-0.3

**Table 6 The relative contribution of natural denudation processes and soil loss from agricultural land for the individual classified sub-regions.**

Region	SSY* (t·km <sup>-2</sup> ·a <sup>-1</sup> )	Relative contribution (%)		Principal denudation processes
		Soil losses from agricultural lands	Natural denudation processes	
Sichuan Hilly Basin	500-600	50-60	40-40	Soil erosion from cultivated lands
Mountain area around the Sichuan Basin	400-500	15-25	75-85	Landslide, scree, rock fall
Karst area	300-400	<5	>95	Bank and gully erosion
Lower Jinsha River mountain area	800-1200	5-10	90-95	Scree, rock fall, slope gully erosion
Hengduan mountain area	500-600	<5	>95	Rock fall, landslide solifluction
Loess Mountain	1000-1500	10-15	85-90	Gully erosion
Qinghai-Tibet Plateau	<200	<1	>99	Bank erosion, solifluction

**Note:** \* indicates mean values during 1954-2005 for river basins with area less than 20,000 km<sup>2</sup>.

load produced in the Upper Yangtze River Basin is sourced from natural denudation processes as an integrated product of concentrated rainstorms, complex landforms and tectonic activities, with the exception of the central Sichuan Hilly area, where soil losses from cultivated hillslopes contribute significantly to fluvial sediment yield. Deforestation is another anthropogenic factor responsible for increasing the denudation rate. It was found that 15%-18% of the forest destruction in the Upper Min River Basin during the 1970s did not significantly influence river discharge (Cheng 1999). Hence, it is unlikely that deforestation notably changes evaporation rates. It is more likely that soil losses increase after logging due to the destruction of vegetation cover that provides soils' resistance to erosion. Thus, the intensity of denudation might be higher within the right-hand tributaries of the Lower Jinsha River due to a dry, hot climate compared with other parts of the Upper Yangtze River. The evaporation intensity increased in given climate conditions after deforestation, which made it more difficult for vegetation to recover and promoted increased physical and chemical weathering. Surface runoff also increased considerably, which lead to an increase in sediment transport from the basin areas to the river channels.

The intensive deforestation of the Upper Yangtze River area began in the 1950s, with a sharp increase in the Lower Jinsha River Basin beginning in the 1960s due to mining and industrial development in the region. For example, the forest coverage in Zhaotong County decreased from 32.8% in the 1950s to 17.5% in 1974 and 14.1% in 1980;

coverage in Dongchuan County went from 30% in the 1950s to 8.9% in the 1980s; and coverage in the Chuxiong Minority went from 55% in the 1950s to 24.1% in the 1980s. Clearly, this has led to an intensification of weathering, gravitational processes and slope gully formation in drainage regions in the southern part of the Lower Jinsha River Basin. As a result, the quantity of sediment delivered from catchment areas increased considerably. For example, the sediment concentration in the upper and lower reaches of the Longchuan River increased 2-2.5 times between the 1960s and the 1980s, with a decrease in water discharge (Figure 10). Serious decreases in water discharge during a given time interval confirms an increase in evaporation due to deforestation (Cheng 1999). Since the 1990s, sediment concentration has been relatively stabilized due to conservation measures (reforestation). Simultaneously, river water discharge has increased (Figure 10). This is a typical situation for southern tributaries of the Lower Jinsha River. A different situation has been observed for the northern tributaries of the Lower Jinsha River, with a relatively high correlation between water discharge and sediment concentration from the 1950s through the beginning of the 2000s (Figure 11). However, some increase in sediment concentration with decreasing water discharge was also observed for a shorter time interval. There are two reasons for the given types of sediment concentration fluctuations. First, a wetter climate compared with southern tributaries has made it much easier for vegetation to recover after logging.

Second, deforestation has not been as intensive in this part of the Lower Jinsha Basin because the majority of industrial and mining plants are located to the south or along the main channel of the Jinsha River. In addition, some fluctuations can be associated with extreme rainstorm events, which prompt a higher proportion of sediment to be delivered to the river channels compared with mean annual values.

The effect of deforestation on the intensification of denudation processes can be found among rivers with a basin area <5000 km<sup>2</sup>. The majority of the sediment produced by denudation processes within catchment areas and transported by debris flows from the first-order catchments to the river valley is re-deposited along pathways to the main transit river. According to the data from a detailed observation in Jiangjia Gully (Xiaojiang River Basin), deposition rates in the lower reach exceed 0.5-1 m per year (Chen et al. 2005). The intensity of sediment deposition on the floodplain of the Xiaojiang River is also very high because the quantity of sediment transported to the valley by debris flows considerably exceeds the transport capacity of the river flow. About 15%-20%

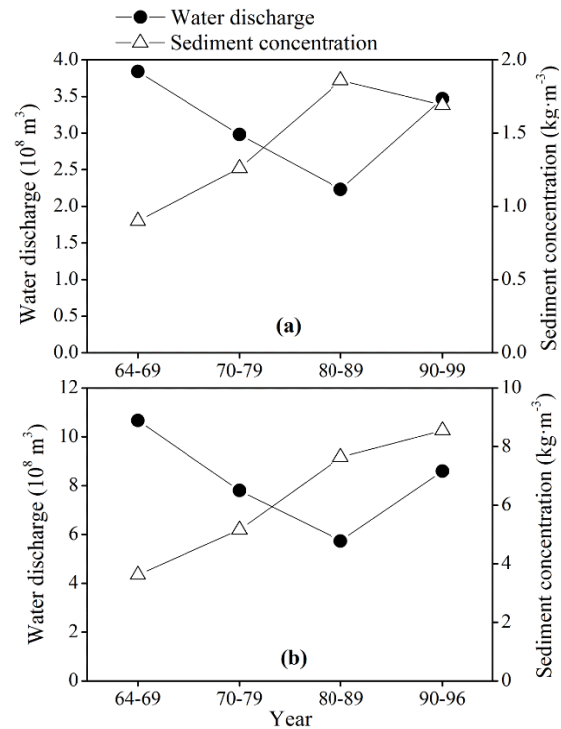


**Figure 10** Dynamic of mean water discharge and sediment concentrations for Longchuan River. (a) **Xiaoheke** station with drainage area of 1788 km<sup>2</sup>; (b) Xiaohuangguayuan station with drainage area of 5560 km<sup>2</sup>.

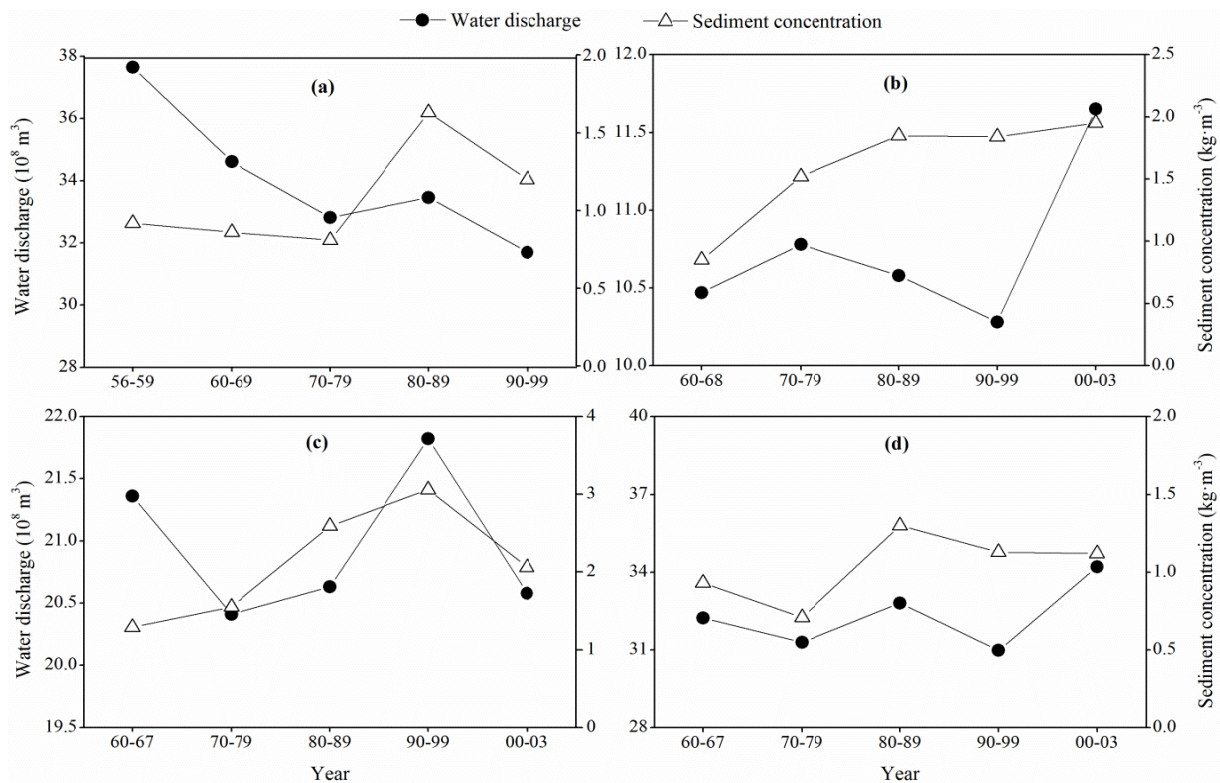


**Figure 11** Dynamic of mean water discharge and sediment concentrations for (a) Manshuiwan station (Anning River) with drainage area of 2620 km<sup>2</sup>; (b) Meigu station (Meigu River) with drainage area of 1607 km<sup>2</sup>; (c) Ningnan station (Heshui River) with drainage area of 3074 km<sup>2</sup>; and (d) Yanrun station (NiuRi River, a tributary of the Min River) with drainage area of 3302 km<sup>2</sup>.

of the sediment transported by debris flows to the Xiao River valley was delivered to the Jinsha River (Dai and Tan, 1996). It is more likely that in reality the proportion of sediment delivered to the Jinsha River is even less. This situation is very typical for the other tributaries of the Lower Jinsha River; however, a detailed analysis of the SSY and water discharges for the tributaries of the Lower Jinsha River confirms the remarkable influence of deforestation on denudation intensification.

During the past decades, implementation of diverse soil conservation measures (e.g., reforestation, terracing, orchards introduction and check dams) has considerably reduced upland soil erosion and denudation rates, particularly in the regions with the highest SSY (e.g., the Sichuan Hilly Basin, the Lower Jinsha Basin and the upper part of the Jialing Basin).

### 3.2 The Volga River Basin

Water erosion on cultivated hillslopes is the predominant land denudation process which gave rise to fluvial sediment fluxes in the Volga River Basin. Major factors influencing the spatial distribution pattern and the magnitude of antropogenic soil erosion are climate, local topography, land cover and land use types.

Intense rainstorm events caused significant soil erosion. Medvedev and Shabaev (1991) measured an erosion occurrence with a magnitude of  $53.5 \text{ t}\cdot\text{ha}^{-1}$  on the Privolzhskaya Upland during the spring of 1974 when rainfall combined with melt-water runoff was observed. About 55 mm of rainfall in the Tula Region (Srednerusskaya Upland) during 2 hours on August 10, 1997 brought about a soil loss of  $22\text{-}59 \text{ t}\cdot\text{ha}^{-1}$  (Belyaev et al. 2008). Such runoff and rainfall events with 10-20 year return periods produce 70%-80% of the total long-term sheet and rill erosion.

Soil erosion intensity in the arable lands of the Volga River Basin varies from 0.1 to  $30 \text{ t}\cdot\text{ha}^{-1}\cdot\text{yr}^{-1}$ . The spatial distribution of the erosion rates for the cultivated hillslopes in the entire basin is presented in Figure 5a and is controlled by numerous factors, of which the most important is a zonal index of rainfall erosivity  $R$  (as used in the USLE). It varies from 3.5-4.0 in the northern part of the basin to 8.0-9.0 in the Srednerusskaya Upland (the western part of the basin). Further south, the values of  $R$  decrease again to about 1.5-2.0 in the lower parts of

the basin. Water storage in snow by the beginning of the snowmelt period is another important parameter influencing soil erosion intensity during spring snowmelt. This is maximal in the northern part of the basin (120-140 mm) and decreases southward to 20-40 mm in the lower part of the basin.

Within climatically uniform territories, local topography is the most important factor controlling soil erosion rates. Large areas with the highest erosion rates occupy the Smolensko-Moskovskaya, Srednerusskaya and Privolzhskaya Uplands and those of the eastern part of the basin, along with the piedmonts of the Urals. The topographical control of erosion is considered in the USLE-based approach by introducing the  $LS$  factor, which incorporates the influence of slope length ( $L$ ) and gradient ( $S$ ) on erosion rates. The northern parts of the Volga River Basin with arable land, dominantly located on uplands and relatively steep valley slopes, are characterized by  $LS$  factor values varying from 1.0 to 2.5. The central part of the basin is characterized by alternation between vast uplands and lowlands, such that the values of the  $LS$  factor decrease. In the southern part of the basin in the Prikaspiyskaya Lowland, a uniformly flat topography with very low slope gradients determines extremely low values of the  $LS$  factor (0.1-0.3).

Soil erodibility  $E$  is a value characterizing soils' susceptibility to erosion, opposite its erosional resistance, which falls under the effect of the unit rainfall erosivity  $R$ . It varies significantly depending mainly on soil texture, humus content and composition. Easily erodible (highest  $E$  values of 4.0-4.5) are soddy, podzolic soils on loessy loams. Similar soils on glacial boulder clays are already less erodible ( $E = 3.0\text{-}3.5$ ). The least erodible soils are humus-rich chernozems with heavy texture and  $E$  values in a range of 0.7-2.0. The erodibility of gray forest soils varies from 1.5 to 3.0 and that of chestnut soils varies from 1.8 to 2.5. Light chestnut soils are characterized by high erodibility ( $E = 3.0$ ).

On the glacial upland landforms the erosion rate reaches  $10\text{-}12 \text{ t}\cdot\text{ha}^{-1}\cdot\text{yr}^{-1}$  while on the glacial-lake and glaciofluvial plains the rate is  $\sim 2 \text{ t}\cdot\text{ha}^{-1}\cdot\text{yr}^{-1}$ . Similar relationships are found between the soil loss from uplands and lowlands, located within the loam loess zone: the Srednerusskaya Upland at 7-8



$t \cdot ha^{-1} \cdot yr^{-1}$  and the Oksko-Donskaya Lowland at  $0.5-2.0 t \cdot ha^{-1} \cdot yr^{-1}$ .

In terms of the contributions made by snowmelt runoff and rainfall to total soil erosion rates, most of the Volga River Basin is characterized by important contributions from both. Snowmelt runoff is responsible for the majority of the average annual soil loss in the northern part of the basin and the northwestern piedmonts of the Urals. To the south, the contribution of rainfall runoff becomes dominant. During the last two decades, water erosion during snowmelt has decreased considerably within the European part of Russia due to warm winters and a sharp decrease in surface runoff during snowmelt (Petelko et al. 2007). In addition, the cultivated lands have decreased considerably, particularly in the forest landscape zone. The Lower Volga and surrounding territories are zones in which water erosion generally decreases significantly due to low the frequency of high-magnitude rainfall events. In those areas, wind erosion becomes the dominant process of sediment redistribution on slope surfaces.

It is well known that the erosion rates in small river catchments are closely related to the percentage of cultivated land (Harvey 2002; Golosov & Panin 2006). This generally increases from north to south, becoming maximal in the steppe zone and decreasing abruptly again toward the semi-desert and desert areas. The so-called patchy cultivation zone is located in the northern part of the basin, where cultivated lands form individual, separate 'islands' in large woodland areas. Under such circumstances, the sediment yield from eroded arable hillslopes does not exert a significant effect on suspended sediment concentrations in river waters, although some individual hillslopes can be severely eroded due to the presence of eroded soils, the sufficient availability of surface water and favorable topography. To the south of the taiga zone the intensity of soil erosion on arable slopes remains high and the percentage of arable land increases. In forest-steppe and steppe zones the highest percentage of arable land is combined with significant potential erosion rates on cultivated slopes. Minimal erosion rates characterize the Prikaspiyskaya Lowland and the southeastern part of the basin.

Generally, the suspended sediment flux in

river is principally contributed by the soil erosion and sediment transport that occur in the southern-central part of the basin, whereas the contribution from the north is relatively minor. Channel bank retreats and bed incisions are the main contributors to suspended sediment in local fluvial systems.

Gully erosion is another contributor to riverine suspended sediment load in the Volga River Basin. The whole basin can be generally divided into four sub-areas (Litvin et al. 2003) according to the genesis and density of gully occurrence (Figure 5b):

1. The belt where gullies represent extremely uncommon and isolated phenomena ( $<2$  gullies/100  $km^2$ ), with no or very low percentage of cultivated land and flat or rolling relief in the northern ( $>57^\circ N - 58^\circ N$ ) part of the forest zone or lowlands with weakly incised valleys  $<10$  m deep.

2. The belt of low gully density varying between 2 and 25 gullies/100  $km^2$  over most of the area. Such areas have relatively low relief range and forested flat interfluves. They occupy the forest zone south of  $57^\circ N - 58^\circ N$ , the flat forested upland areas of the Smolensko-Moskovskaya and Srednerusskaya Uplands and part of the Oksko-Donskaya Lowland. In the southern part of the forest zone, gully density gullies can reach 25-50/100  $km^2$ . Most of the gullies presently found in forests were formed during periods of much wider expansion in the cultivation of former arable lands.

3. The main belt of gulying in the forest-steppe and steppe zones. The main anthropogenic factor in gully formation here is the cultivation of almost the entire area. Gulying is also promoted by favorable natural conditions such as substantial volumes of melt water and rainfall, relatively erodible loessy subsoil parent materials and a relatively high topographical range. When these areas were first cultivated, intensive tillage led to the formation of gully systems of the greatest extent and density, compared to other regions. The topographical range and land use pattern differentiate the gully density within the belt. Areas with moderate gully density (25-50/100  $km^2$ ) typically occupy relatively flat interfluves and uplands with low topographic range (the Smolensko-Moskovskaya Upland), in addition to lower rolling plains (the Tambov Range, the Oksko-Donskaya Lowland and the western part of the Obshchiy Syrt Upland). Areas of advanced agricultural development with relatively favorable natural conditions for gully formation are

characterized by deeply dissected relief and high gully density (50-100/100 km<sup>2</sup>). Such regions include the central parts of the upland country such as the Srednerusskaya and Privolzhskaya Uplands. Areas with very high gully density (>100/100 km<sup>2</sup>) are found in a relatively small region in the middle of the upland country and along the steep slopes of the main valleys, comprising <10% of the entire territory affected by gully erosion.

4. The southern belt with very low gully density. This region includes the greater part of the Prikaspiyskaya Lowland.

Kosov (1970) collected more than 300 gully growth-rate measurements in the European part of the former USSR for various land use types (Table 7). About 45% of these data show gully growth over 1-5 years, 35% show growth up to 10 years and the others for longer periods up to 170 years. The gullies on arable land are characterized mainly by medium growth (50% of the gullies have a maximum growth rate <5 m·yr<sup>-1</sup>). Catastrophic (>100 m·yr<sup>-1</sup>) rates of gully development are more typical in the areas of forest cutting and industrial development.

Despite strong fluctuations in gully headcut retreat rates between individual years, their tendency to decrease is observed in most of the long-cultivated regions of the Volga River Basin (Rysin 1998). It should be noted, however, that this tendency is most applicable for gullies being developed on former arable land for relatively long periods (up to 200-300 years) and presently reaching a quasi-stable state. There are, in contrast, areas in which new (and therefore very active) gullies are being formed, mainly as a result of the negative effects of human activities and current land use changes. Large stabilized gullies can also develop active branches if there are catchment areas available (Litvin et al. 2003).

In addition to the internal gully system threshold of reaching the minimal headcut catchment area, other reasons for the observed tendency are as follows: 1) the positive effects of

soil conservation measures applied in the 1950s-1980s; 2) a general decrease in arable areas from the 1990s-2000s; 3) a shift to more soil-protective crop rotations with a high percentage of perennial grasses from the 1990s-2000s; and 4) a decrease in surface runoff irregularity (lower extremes), snowmelt intensity and snowmelt runoff discharges from the 1990s-2000s.

The SSC map shows five area categories (Figure 6a) based on the changes in typical SSC values. The boundaries of these areas were drawn to consider the spatial patterns of surface lithology and soil cover in the Volga River Basin. The lowest SSC (<50 g·m<sup>-3</sup>) characterizes the rivers of the upper Volga Basin, those north of the northwestern part of the Oka River Basin, the left-hand tributaries of the middle Volga River, the rivers of the middle Vyatka River Basin and those in the northern part of the Kama River Basin. The areas of lowest SSC form an almost continuous belt across the northern part of the Volga River Basin, with an irregular southern boundary. The lowest SSC values are also observed for the rivers in the eastern part of the Kama River Basin flowing from the Ural Mountains and their foothills. In general, this zone is limited to forest with soddy podzolic soils, and to mountainous regions. This area is characterized by a low area of arable lands (<20%-30%), so it is likely that the bank and bottom erosion of the river channels are the main sources of sediment. South of the above zone there are few separated areas characterized by SSC values in a range from 50-100 g·m<sup>-3</sup>. The territories characterized by SSC values in a range of 100-200 g·m<sup>-3</sup> are located in the southern forest-steppe part of the Oka River Basin (the Srednerusskaya Upland), the central and southern parts of the Kama River Basin (dissected upland areas of the Ufimskoe Plateau and Sarapulskaya, Bugulmino-Belebeevskaya, Verhnekamskaya and Vyatskiy Uval Uplands). All of these areas are characterized by a high percentage of arable land (40%-60% and

**Table 7 Distribution of gullies with different growth rates in the Volga River Basin (Kosov 1970)**

Land uses	Total gully number	Maximum annual (seasonal) growth				
		<5 m	6-15 m	20-40 m	50-80 m	>100 m
Agriculture	269	50%	25%	15%	8%	2%
Logging	15	25%	18%	25%	7%	25%
Road building	17	15%	25%	30%	25%	5%
Industrial development	19	20%	20%	25%	10%	25%

higher) and a high risk of soil erosion.

The steppe areas along the lower Volga River typically have higher SSC values, from 200-500  $\text{g}\cdot\text{m}^{-3}$  (Figure 6a). A high SSY can be explained by the intensive cultivation of upland landscapes. Areas with even higher SSC values include the Mesha River Basin (interfluvium between the Volga and Kama Rivers), the small rivers of the Privolzhskaya Upland and the upper reaches of the Buzuluk, Samara, Tok, Sok and Bolshoy Kinel Rivers with a high proportion of cultivated lands and high relative relief (Chalov and Shtankova 2003).

The spatial distribution of the SSY values generally resembles that of the SSC values, although the pattern is somewhat more mosaic (Figure 6b). There is a general tendency of increase in the SSY values from north to south, a dynamic that is most evident within the Kama River Basin, which has quasi-longitudinal elongation through a number of landscape zones from taiga to dry steppes. In the Oka River Basin that tendency is rather unclear because it is located entirely in the southern part of the forest zone, which is elongated in a quasi-latitudinal direction. Most of the rivers in the upper Volga Basin are characterized by the lowest SSY values.

The variety of conditions influencing sediment mobilization and routing in the western part of the Volga River Basin (mainly in the Oka River Basin) is reflected in changes in the SSY values along the larger rivers (Figure 6b). Along the Oka River, the SSY values decrease downstream as it receives tributaries (the Zhizdra and Ugra Rivers and the rivers of the Mecherskaya Lowland) due to low suspended sediment concentrations. Along the Moksha River, the SSY values also initially decrease downstream (toward the central part of the Oksko-Donskaya Lowland), but then increase further downstream. Along the Klyazma River, the SSY values initially increase downstream as the river flows through the Vladimirovskoe Opolye with its high proportion of arable lands, and then begin to fall once the river leaves the actively eroded areas.

In the Kama River Basin, the highest SSY values (30-40  $\text{t}\cdot\text{km}^{-2}\cdot\text{yr}^{-1}$ ) are found in the central and lower parts, including the upper and lower parts of the Vyatka River Basin and most of the Belaya River Basin. The lowest values (<10  $\text{t}\cdot\text{km}^{-2}\cdot\text{yr}^{-1}$ ) correspond to the mountainous areas and the

central parts of the Bugulmino-Belebeevskaya Upland with a low proportion of cultivated lands. Intermittent SSY values are observed in the northern part of the Kama River Basin under the taiga forests and the slopes of the Bugulmino-Belebeevskaya Upland toward the Kuibyshevskoe Reservoir on the Volga River.

In the lower part of the Volga River Basin, the left-hand tributaries flow through the lowland areas while the right-hand tributaries descend from the short, steep slopes of the Privolzhskaya Upland. Consequently, the latter are characterized by higher SSY values (20-30  $\text{t}\cdot\text{km}^{-2}\cdot\text{yr}^{-1}$ ) in the Tereshka River and the middle reach of the Sviyaga River. On the left side of the basin, however, there is also a localized area of very high SSY values (40-60  $\text{t}\cdot\text{km}^{-2}\cdot\text{yr}^{-1}$ ), most likely associated with local geomorphological factors (more dissected topography). This area of high SSY values coincides with a zone of maximum SSC values (upper reaches of the Samara, Bolshaya Kinel and Sok Rivers). The low reach of the Sviyaga River and the entire Mesha River are characterized by absolutely maximal SSY values (>60  $\text{t}\cdot\text{km}^{-2}\cdot\text{yr}^{-1}$ ), in accordance with maximum SSC values.

The lowest (<5  $\text{t}\cdot\text{km}^{-2}\cdot\text{yr}^{-1}$ ) SSY values are typical for the rivers in the upper part of the Volga River Basin and those in the central part of the Oka River Basin. In the eastern part of the Volga River Basin (mainly in the Kama River Basin) such low SSY values have not been observed, while maximum SSY values (>40  $\text{t}\cdot\text{km}^{-2}\cdot\text{yr}^{-1}$ ) have been observed on the steppes of the lower part of the Volga River Basin (Chalov and Shtankova 2003).

A clear trend of decreasing SSY in most rivers in the Volga Basin has been observed during last two decades, which can be ascribed to the rapid growth of abounded cultivated lands within the Central part of the Volga River basin (Belyaev et al. 2009) and increases in winter temperature, which have decreased surface runoff during snowmelt (Petelko et al. 2007). Also it leads to decreasing of soil losses, gully growth and sediment transport from the basin areas to the river channels.

#### 4 Conclusion

By assembling the available data of soil erosion on cultivated and uncultivated hillslopes

and decoupling with the natural and anthropogenic controlling factors operating on the individual denudation processes, this paper subdivided the whole Upper Yangtze River Basin into seven sub-regions with different proportional inputs of principal denudation processes into fluvial suspended sediment yields. Natural factors comprising topography, climate, lithology and tectonic activity are responsible for the spatial variations in denudation rates across the basin.

However, land use change due to deforestation and land reclamation has played an important role in the intensification of sediment production in the Upper Yangtze River Basin. In particular, in the most densely-populated Sichuan Hilly Basin with a cultivated land ratio exceeding 50%, soil losses from cultivated lands are the main source area for sediment production. The influence of deforestation affected the Lower Jinsha River Basin, especially the southern part of this area where deforestation intensity and denudation processes increased considerably due to unfavorable climate conditions for vegetation recovery. The application of national soil conservation programs during the recent decades promoted a significant reduction in soil losses and sediment production. However, the same effect is difficult to achieve among the tributaries of the Lower Jinsha River due to the huge amount sediment accumulated in the river valley bottoms and re-mobilized through river channel migration.

In the Volga River Basin, anthropogenic sheet, rill and gully erosion are the predominant

denudation processes in the southern part. The bank and bottom erosion of the river channels is the main source of sediment in the northern part of the Volga River Basin where the SSY is considerably lower than that in the southern part. The proportion of cultivated lands is the key parameter controlling denudation intensity within the basin. However, local relief characteristics also considerably influence erosion rates and SSY in the southern half of the Volga River Basin. Lithology, soil cover and climate conditions are determined by the spatial distribution of sheet, rill and gully erosion intensity, but they play a secondary role in SSY spatial distribution.

Finally it is possible to conclude that natural denudation processes are mostly responsible for high SSY in the Upper Yangtze River basin. The opposite situation is observed in the Volga River basin, where a high proportion of cultivated lands in the southern half of the basin lead to intensive sheet, rill and gully erosion in particular within uplands. Intensity of basin erosion is comparable with that observed in the Upper Yangtze River basin, which is recently well-known as the area with one of the highest erosion rates.

## Acknowledgements

Financial support for this study was jointly provided by the Chinese Academy of Sciences (No. ZCX2-XB3-09) and the Ministry of Science and Technology of China (No. 2011BAD31B03).

## References

- Belyaev VR, Golosov VN, Kisenko KS, et al. (2008) Combining direct observations, modelling and <sup>137</sup>Cs tracer for evaluating individual event contribution in long-term sediment budgets. *Sediment Dynamics in Changing Environments* (Proceedings of a symposium held in Christchurch, New Zealand, December 2008). IAHS Publ. No. 325, 114-122.
- Belyaev VR, Golosov VN, Kuznetsova JS, et al. (2009) Quantitative assessment of effectiveness of soil conservation measures using a combination of <sup>137</sup>Cs radioactive tracer and conventional techniques. *Catena* 79: 214-227.
- Chalov RS, Shtankova NN (2003) Sediment yield, contribution of bedload sediment and its reflection in channel morphological patterns in rivers of the Volga River Basin. In: *Problems of river channel investigations*. Vol. 9. pp 195-205. Moscow University Publ., Moscow, Russia (In Russian).
- Chen J, He YP, Wei FQ (2005) Debris flow erosion and deposition in Jiangjia Gully, Yunnan, China. *Environmental Geology* 48: 771-777.
- Chen XQ (1996) An integrated study of sediment discharge from the Changjiang River, China and the delta development since the Mid-Holocene. *Journal of Coastal Research* 12(1): 26-37.
- Cheng GW (1999) Forest change: hydrological effects in the Upper Yangtze River valley. *Ambio* 28: 457-459.
- Dai D, Tan Y (1996) Soil erosion and sediment yield in the Upper Yangtze River basin. *Erosion and Sediment Yield: Global and Regional Perspectives* (Proceedings of the Exeter Symposium, July 1996). IAHS Publ. no. 236, pp 191-203.
- Edmond JM, Palmer MR, Measures CI, et al. (1995) The fluvial geochemistry and denudation rate of the Guayana Shield in Venezuela, Colombia and Brazil. *Geochimica Cosmochimica Acta* 59: 3301-3325.
- Fan J, Morris G (1992) Reservoir sedimentation II: reservoir desiltation and long-term storage capacity. *Journal of Hydraulic Engineering* 118(3): 370-384.
- Gao P (2008) Understanding watershed suspended sediment transport. *Progress in Physical Geography* 32(3): 243-263.

- Gavrilova IP, Bogdanova MD (1998) Distribution and geochemical regime of the main soil types. Alexeevsky NA (Ed.) Small Rivers Volga Basin. Moscow State University: pp 48-63 (In Russian).
- Golosov VN (2006) Influence of different factors on the sediment yield of the Oka basin rivers (central Russia). In: Rowan JS, Duck RW, Werritty A (eds.) Sediment Dynamics and the Hydromorphology of Fluvial Systems, IAHS Publ 306, pp 28-36.
- Golosov VN, Panin AV (1988) Scree processes at gully slopes in the western Tien-Shan mountains. *Geomorphologiya* 3: 46-50 (In Russian).
- Golosov VN, Panin AV (2006) Century-scale stream network dynamics in the Russian Plain in response to climate and land use change. *Catena* 66: 74-92.
- Harvey AM (2002) Effective timescales of coupling within fluvial systems. *Geomorphology* 44: 175-201.
- He YP, Xie H, Cui P, et al. (2003) GIS-based hazard mapping and zonation of debris flows in Xiaojiang Basin, southwestern China. *Environmental Geology* 45: 286-293.
- Higgitt DL, Lu XX (2001) Sediment delivery to the three gorges: 1. Catchment controls. *Geomorphology* 41: 143-156.
- Instruction on calculating hydrological characteristics for planning counter-erosion measures in the European area of the USSR. 1979. *Gidrometeoizdat Publ., Leningrad, Russia*. p 61. (In Russian)
- Jin Y, Wang F, Sun P (2009) Landslide hazard triggered by the 2008 Wenchuan earthquake Sichuan, China. *Landslides* 6: 139-151.
- Kosov BF(1970) Gully growth on USSR territory. *Eroziya pochv I ruslovye process* 1:23-34. (In Russian)
- Larionov GA. (1993) Water and wind erosion: the main principles and quantitative estimates. *Izd-vo Mosk. University, Moscow*. p 236. (In Russian)
- Li S, Lobb DA, Lindstrom MJ, et al. (2007) Tillage and water erosion on different landscapes in the northern North American Great Plains evaluated using <sup>137</sup>Cs technique and soil erosion models. *Catena* 70: 493-505.
- Lin C, Tu S, Huang J, et al. (2009) The effect of plant hedgerows on the spatial distribution of soil erosion and soil fertility on sloping farmland in the purple-soil area of China. *Soil and Tillage Research* 105: 307-312.
- Litvin LF (2002) Geography of soil erosion on agricultural lands of Russia. *IKC Akademkniga, Moscow*, p.255.
- Litvin LF, Zorina EF, Sidorchuk AY, et al. (2003) Erosion and sedimentation on the Russian Plain. Part 1: contemporary processes. *Hydrological Processes* 17: 3335-3346.
- Mabit L, Benmansour M, Walling DE (2008) Comparative advantages and limitations of fallout radionuclides (<sup>137</sup>Cs, <sup>210</sup>Pb and <sup>7</sup>Be) to assess soil erosion and sedimentation. *Journal of Environmental Radioactivity* 99: 1799-1807.
- Medvedev IF, Shabaev AI (1991) Erosion processes on arable lands of Privolzhskaya upland. *Pochvovedenie* 11: 61-69. (In Russian)
- Palmieri A, Shan F, Dinar A (2001) Economics of reservoir sedimentation and sustainable management of dams. *Journal of Environmental Management* 61: 149-163.
- Peng T, Wang SJ (2012) Effects of land use, land cover and rainfall regimes on the surface runoff and soil loss on karst slopes in southwest China. *Catena* 90: 53-62.
- Petelko AI, Golosov VN, Belyaev VR (2007) Experience of design of system of counter-erosion measures. Proceedings of the tenth international symposium on river sedimentation. Vol. 1. Moscow. pp 141-149.
- Porto P, Walling DE, Callegari G (2011) Using <sup>137</sup>Cs measurements to establish catchment sediment budgets and explore scale effects. *Hydrological Processes* 25: 886-900.
- Qi YQ, Zhang XB, He XB (2006) A study on soil erosion induced sediment yield by reservoir and pond deposits dating with <sup>137</sup>Cs in small catchments of the hilly Sichuan Basin and the Three Gorges Region. *Geographical Research* 25(4): 641-647. (In Chinese with English abstract).
- Qin J, Huh Y, Edmond JM, et al. (2006) Chemical and physical weathering in the Min Jiang, a headwater tributary of the Yangtze River. *Chemical Geology* 227: 53-69.
- Quine T, Walling DE, Zhang XB (1999) Tillage erosion, water erosion and soil quality on cultivated terraces near Xifeng in the Loess Plateau, China. *Land Degradation and Development* 10: 251-274.
- Ritchie JC, McHenry JR (1990) Application of radiation fallout <sup>137</sup>Cs for measuring soil erosion and sediment accumulation rates and patterns: A review. *Journal of Environmental Quality* 19: 215-233.
- Rysin II (1998) Gully erosion in Udmurtiya. *Izhevsk, Izd-vo Udmurt. University*. (In Russian)
- Schuller P, Walling DE, Sepulveda A, et al. (2004) Use of <sup>137</sup>Cs measurements to estimate changes in soil erosion rates associated with changes in soil management practices on cultivated land. *Applied Radiation and Isotopes* 60: 759-766.
- Shi DM (1998) Analysis relationship between soil and water losses and flood disaster in Yangtze River basin. *Journal of Soil and Water Conservation* 5: 1-7. (In Chinese with English abstract).
- Su ZA, Zhang JH, Nie XJ (2010) Effect of Soil Erosion on Soil Properties and Crop Yields on Slopes in the Sichuan Basin, China. *Pedosphere* 20(6): 736-746.
- Sutherland RA (1992) Caesium-137 estimates of erosion in agricultural areas. *Hydrological Processes* 6: 215-225.
- The Office of Soil and Water Conservation Committee of Sichuan Province (1991) *Compilation of Experiment and Observation Results of Soil and Water Conservation in Sichuan Province*. (In Chinese)
- Tiessen KHD, Li S, Lobb DA, et al. (2009) Using repeated measurements of <sup>137</sup>Cs and modeling to identify spatial patterns of tillage and water erosion within potato production in Atlantic Canada. *Geoderma* 153: 104-118.
- Walling DE, Fang D (2003) Recent trends in the suspended sediment loads of the world's rivers. *Global and Planetary Change* 39: 111-126.
- Walling DE, Golosov VN, Panin AV, et al. (2000) Use of radiocaesium to investigate erosion and sedimentation in areas with high levels of Chernobyl fallout. In: Foster IDL (Ed.) *Tracers in Geomorphology*. John Wiley and Sons, Chichester, pp 183-201.
- Walling DE, He Q, Blake W (1999) Use of <sup>7</sup>Be and <sup>137</sup>Cs measurements to document short- and medium-term rates of water induced erosion on agricultural land. *Water Resources Research* 35: 3865-3874.
- Wang SJ, Liu QM, Zhang DF (2004) Karst rocky desertification in southwestern China: geomorphology, land use, impact and rehabilitation. *Land Degradation and Development* 15: 115-121.
- Wang YK, Wen AB, Zhang XB (2003) Study of Soil Erosion on Cultivated Slope Land in Severe soil Loss Regions of Upper Reaches of Yangtze River Basin Using <sup>137</sup>Cs Technique. *Journal of Soil and Water Conservation* 17(2): 77-80. (In Chinese with English abstract).
- Wen AB, Zhang XB, Wang YK, et al. (2002) Study on soil erosion rates using <sup>137</sup>Cs technique in Upper Yangtze River. *Journal of Soil and Water Conservation*. (In Chinese with English abstract)
- Wen AB, Qi YQ, Wang YC (2005) Study on Erosion and Sedimentation in Yangtze Three Gorge Region. *Journal of Soil and Water Conservation* 19(2): 33-36. (In Chinese with English abstract)
- Wen AB, Zhang XB, Li H (2008) Interpreting variations of <sup>137</sup>Cs, <sup>210</sup>Pb<sub>ex</sub> and fine particle contents in a deposit profile of the Jiulongdian Reservoir, Chuxiong, Yunnan, China. *Journal of Sediment Research* 6: 17-23. (In Chinese with English abstract)
- Wen AB, Zhang XB, Wang YK (2011) A Study on Soil Erosion Rates of the Purple Slope Cultivated Land Using Caesium-137 Technique in the Upper of the Yangtze River, *Journal of Mountain Science* 19(S): 56-59.

- Wu W, Yang J, Xu S, et al. (2008) Geochemistry of the headwaters of the Yangtze River, Tongtian He and Jinsha Jiang: Silicate weathering and CO<sub>2</sub> consumption. *Applied Geochemistry* 23: 3712-3727.
- Yang D, Kanae S, Oki T, et al. (2003) Global potential soil erosion with reference to land use and climate changes. *Hydrological Processes* 17: 2913-2928.
- Yang JL, Zhang CL, Shi XZ, et al. (2009) Dynamic changes of nitrogen and phosphorus losses in ephemeral runoff processes by typical storm events in Sichuan Basin, Southwest China. *Soil and Tillage Research* 105: 292-299.
- Yang S, Jung HS, Li C (2004) Two unique weathering regimes in the Changjiang and Huanghe drainage basins: Geochemical evidence from river sediments. *Sedimentary Geology* 164: 19-34.
- Yin H, Li C, Chen D, et al. (1998) Problems and countermeasures on the flood control of middle Yangtze River. *Proceedings of the Symposium of Resources, Environment and Sustainable Development of Central China and Hubei Province, Wuhan. China University. Geosciences Press.* pp 1-7. (In Chinese with English abstract)
- Zhang XB, Bai XY, Liu XM (2011) Application of <sup>137</sup>Cs fingerprinting technique to interpreting responses of sediment deposition of a karst depression to deforestation in the catchment of the Guizhou Plateau, China. *Science China* 41(2): 265-271.
- Zhang XB, Long Y, He XB, et al. (2008) A simplified <sup>137</sup>Cs transport model for estimating erosion rates in undisturbed soil. *Journal of Environmental Radioactivity* 99(8): 1242-1246.
- Zhang XB, Quine TA, Walling DE (1998) Soil erosion rates on sloping land on the Loess Plateau near Ansai, Shanxi Province, China: an investigation using <sup>137</sup>Cs and rill measurements. *Hydrological Processes* 12: 171-189.
- Zhang XB, Wen AB (2002) Variations of sediment in upper stream of Yangtze River and its tributary. *SHUILI XUEBAO* 4: 56-59. (In Chinese with English abstract)

**Lily 一校:** **Table 1,2 和 3** 中的分隔线在排版的时候丢失了, 已经全部加上, 请作者确认的时候仔细检查分隔线上下的内容是否正确。**Table 2 和 3** 中蓝色高亮显示的表头缩写了, 然后在 **Note** 中加以说明了, 请作者确认是否合适。第 **13** 页 **Figure 8** 图题中的“**Figure 8A**”是什么意思? 请作者检查并修改。**Table 2** 中的表头“**Aver. value**”上方多余的一个表头“**No. of profile**”我删去了, 请作者确认是否正确。第 **10** 页公式 (1) 下面一段中红色高亮显示的数字和单位请作者检查是否正确。图 **9** 中左边总有一条竖着的黑线, 我改不了, 排版之前的样本中没有黑线, 把这个图拷过来就有黑线了, 请作者确认的时候重新提供这个图的 **TIF** 文件吧!

**吴二校:** **table 1** 有些问题, 已在表中写明; **table 2,3** 表中内容不多, 但是占的版面很大, 如果调整一下的话应该可以减少一页, 看有必要没有。文献有些格式不对, 已修改。

**Lisa 三校:** 首页信封已改。表 **4** 和表 **6** 个别行增加了行间距以便能看清。参考文献格式小问题较多, 已改。

**QIU:**

1. **Figure 1 and Figure 2** 的大小比例不合适, 重新调整, 使版式更美观;
2. **Table 2** 两页的横表重新进行修改设计后, 变成了一页的表格。请作者着重检查一下这个表格;
3. 所有表格重新调整, 便于阅读。
4. 调整了整个版面。目前已由 **23** 页变成 **22** 页。